Electronic Supporting Information

Impact of Mg^{2+} and Zn^{2+} substitution on the structure, magnetic anisotropy and magnetostriction of $NiFe_2O_4$

M. Satish [a], H. M. Shashanka [a], Sujoy Saha [b], V. R. Reddy[c], B. Sahoo*[d], P. N. Anantharamaiah*[a]

[a]*Department of Chemistry, Faculty of Natural Sciences, M. S. Ramaiah University of Applied Sciences, Bengaluru-560058, India*

[b]*Department of Basic Sciences, School of Sciences and Humanities, SR University, Warangal-506371, India*

[c]*UGC-DAE Consortium for Scientific Research India, University Campus, Khandwa Road, Indore 452001, India*

[d]*Materials Research Centre, Indian Institute of Science, Bengaluru-560012, India*

E-mail: anantharamaiah.cy.mp@msruas.ac.in

bsahoo@iisc.ac.in

Table S1: List of maximum magnetostriction strain (λ_{max}) values reported for the sintered polycrystalline NFO and its derivative samples. All these values are along the longitudinal direction.

Compositions	Synthesis method	Sintering temperature (°C) and time	λ_{max} (ppm)	H @ λ_{max} (kOe)	Reference*
$NiFe_2O_4$	Spark plasma sintering	1000;1h	-37	∽2	R1
$NiFe_2O_4$	Sol-gel	1200; 12h	-27	∽4	R2
$NiFe_2O_4$	Tartrate-gel	1200; 2h	-25	∽1.7	R3
$NiFe_2O_4$	Autocombustion	1200; 2h	-35	∽3	R4
$Ni_{0.75}Zn_{0.25}Fe_{1.8}O_4$	Sol-gel	1200; 12h	-20	∽4	R2
$Ni_{0.50}Zn_{0.50}Fe_{1.8}O_4$	Sol-gel	1200; 12h	-9	∽4	R2
$Ni_{0.75}Cu_{0.25}Fe_{1.8}O_4$	Autocombustion	1200; 2h	-24	∽1.3	R5
$Ni_{0.50}Cu_{0.50}Fe_{1.8}O_4$	Autocombustion	1200; 2h	-34	∽1.7	R5
$NiMg_{0.2}Fe_{1.8}O_4$	Tartrate-gel	1200; 2h	-22	∽3.1	R3
$NiIn_{0.2}Fe_{1.8}O_4$	Tartrate-gel	1200; 2h	-25	∽1.5	R3
$NiGa_{0.25}Fe_{1.75}O_4$	Autocombustion	1200; 2h	-28	∽3	R6
$NiGa_{0.50}Fe_{1.50}O_4$	Autocombustion	1200; 2h	-22	∽3	R6
$NiFe_{1.95}Nd_{0.05}O_4$	Solid state	1250; 12h	-25	∽3.5	R7
$NiFe_{1.95}Gd_{0.05}O_4$	Solid state	1250; 12h	-27	∽4.5	R7

References:

R1. Alex Aubert; Vincent Loyau; Frédéric Mazaleyrat; Martino LoBue, IEEE Transactions on Magnetics 57, 2021, 2501105

R2. M. Atif, M. Nadeem, R. Grössinger, and R. S.Turtelli, *J. Alloys Compd.*, 2011, **509,** 5720-5724.

R3. P. N. Anantharamaiah, B. P. Rao, H. M. Shashanka, J. A. Chelvane, V. Khopkar, and , B. Sahoo, *Phys. Chem. Chem. Phys.*, 2021, **23**, 1694-1705

R4. M. Satish, H. M. Shashanka, S. Saha, K. Haritha, D. Das, P. N. Anantharamaiah, and C.V. Ramana, *ACS Appl. Mater. Interfaces*, 2023, **15**, 15691-15706.

R5. M. Satish, H. M. Shashanka, S. Saha, S., D. N. Singh, and P. N. Anantharamaiah, *J. Magn. Magn. Mater.* 2023, **585**, 171113.

R6. H. M. Shashanka, D. N. Singh, J. A. Chelvane, and P. N. Anantharamaiah, 2024. *Inorg. Chem. Commun.*, 2024, **161**, 112029.

R7. K. K Bharathi, J. A. Chelvane, and G. Markandeyulu, 2009. Magnetoelectric properties of Gd and Nd-doped nickel ferrite. *J. Magn. Magn. Mater.*, 2009, **321**, 3677-3680.

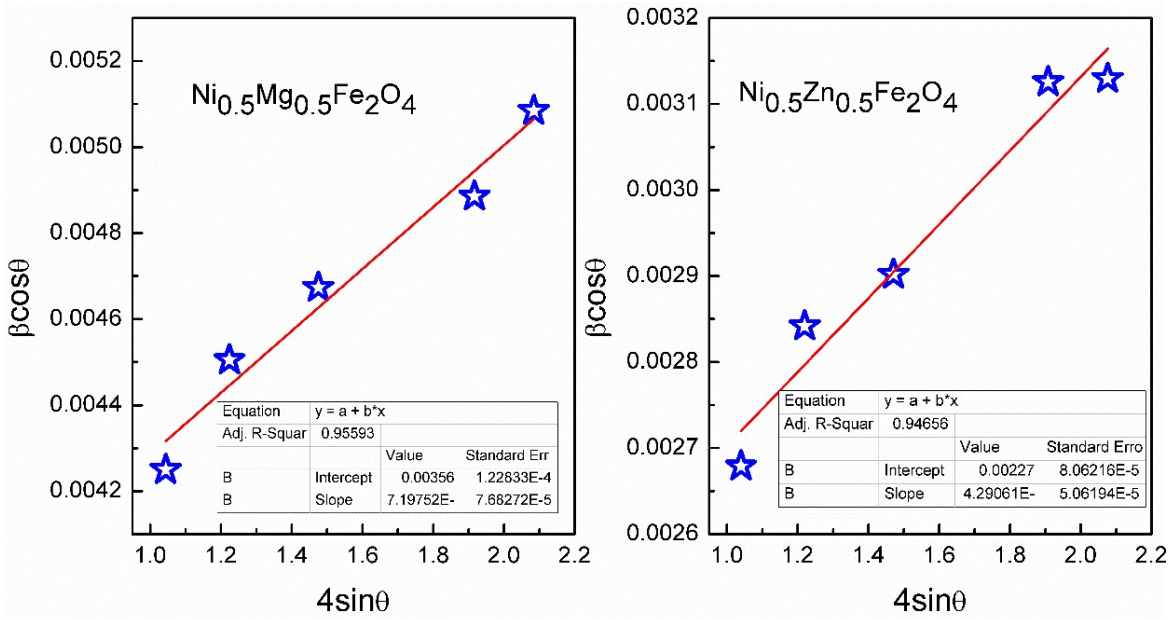

Fig. S1. Williamson-Hall plots for the as-synthesized $Ni_{0.5}Mg_{0.5}Fe_2O_4$ and $Ni_{0.5}Zn_{0.5}Fe_2O_4$ samples.

Table S2. Average crystallite size (D_v), strain (ε), lattice parameter (a) and theoretical density (ρ) of the as-synthesized $Ni_{1-x}Mg_xFe_2O_4$ series of samples.

Sample	'D_v' (nm)	ε_{strain} x 10^{-4}	'a'(Å)	$\rho_{theor.}$ (g/cm^3)
x=0	69	4.32	8.345	5.356
x=0.25	40	2.59	8.346	5.158
x=0.5	39	7.19	8.347	4.960
x=0.75	36	9.19	8.358	4.746
x=1	33	11.5	8.372	4.526

Table S3. Average crystallite size (D_v), strain (ε), lattice parameter (a) and theoretical density (ρ) of the as-synthesized $Ni_{1-x}Zn_xFe_2O_4$ series of samples.

Sample	'D_v' (nm)	ε_{strain} x 10^{-4}	'a'(Å)	$\rho_{theor.}$ (g/cm^3)
x=0	69	4.32	8.345	5.356
x=0.25	52	7.12	8.355	5.375
x=0.5	61	4.29	8.374	5.377
x=0.75	62	2.98	8.396	5.372
x=1	63	4.29	8.424	5.349

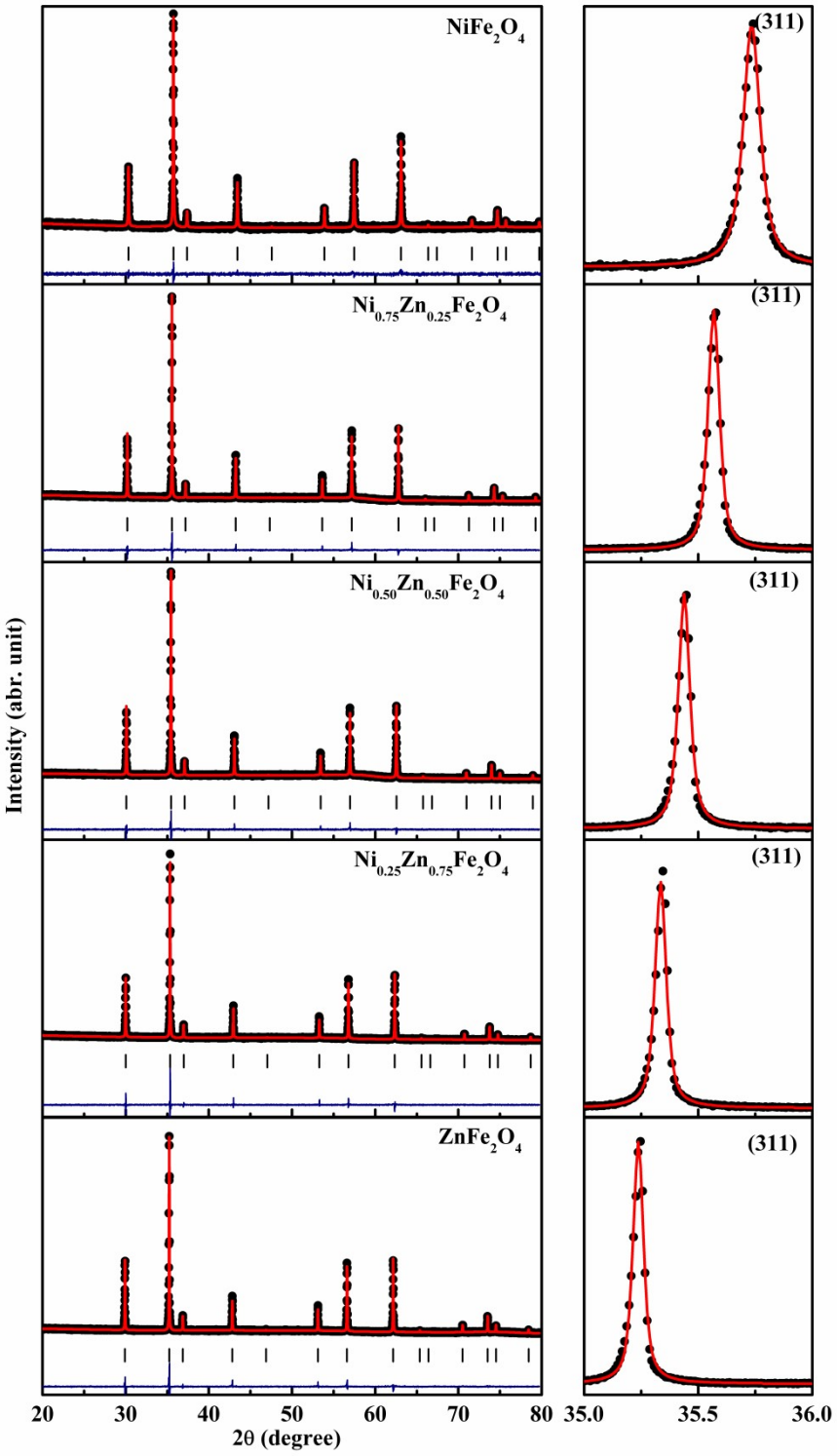

Fig. S2. Rietveld fit XRD patterns of sintered Zn-substituted $NiFe_2O_4$ samples shown in the left panel. Variation in the 311 peak postion with increasing the Zn content is shown in the right panel.

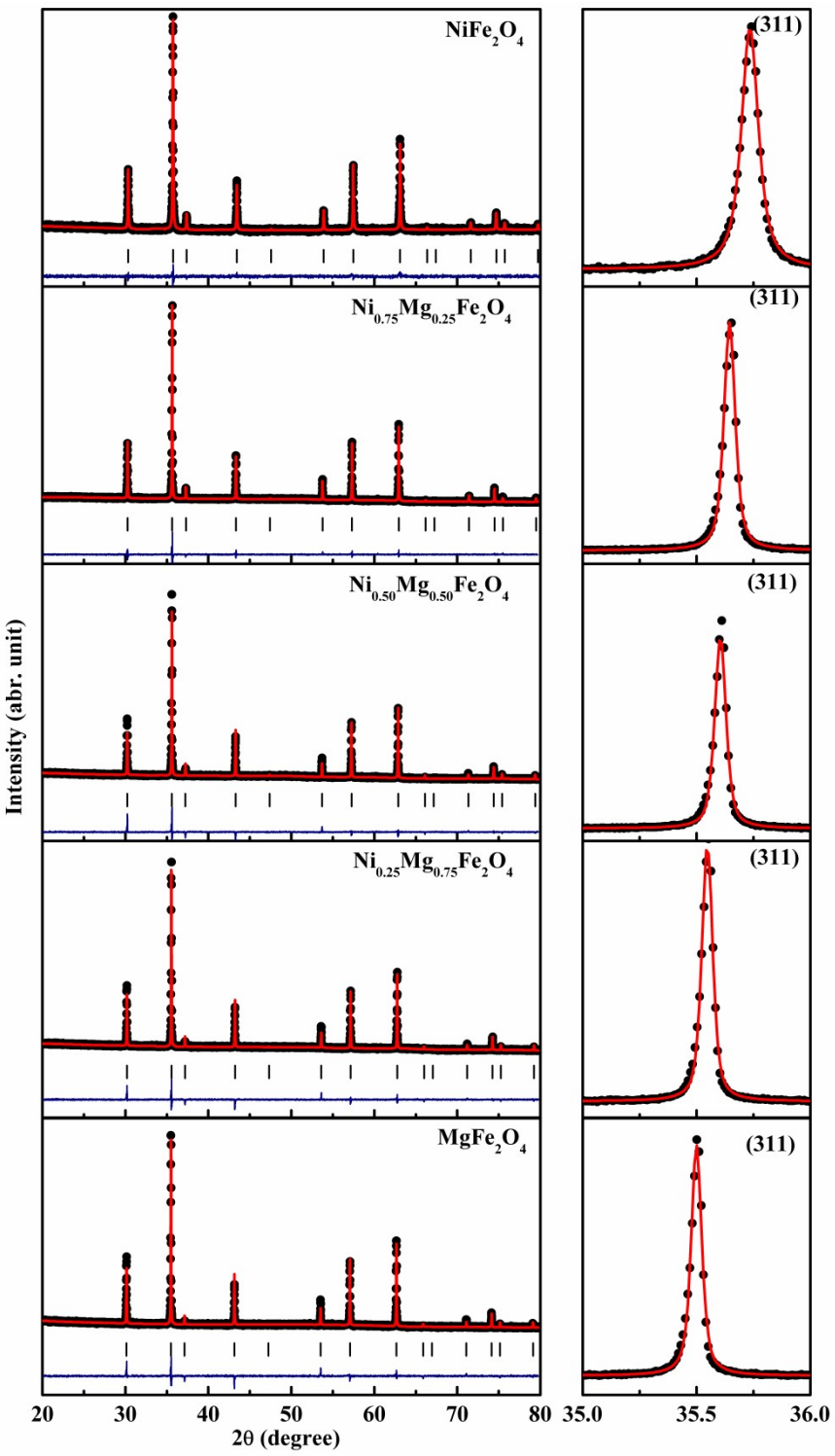

Fig. S3. Rietveld fit XRD patterns of sintered Mg-substituted $NiFe_2O_4$ samples shown in the left panel. Variation in the 311 peak postion with increasing the Mg content is shown in the right panel.

Table S4. Refined lattice constants, atomic parameters and isotropic thermal parameters of the $Ni_{1-x}Zn_xFe_2O_4$ (x = 0, 0.25, 0.50 0.75 and 1.0).

	$x = 0$	$x = 0.25$	$x = 0.5$	$x = 0.75$	$x = 1.0$
a (Å)	8.32665	8.36429	8.39397	8.41766	8.44032
B_{iso} (A site)	0.761	1.281	1.241	1.312	1.121
B_{iso} (B site)	0.761	1.273	1.159	1.190	0.887
O (x, x, x)	0.25557	0.25944	0.26074	0.26126	0.26178
R_p	2.10	1.79	1.80	1.94	1.96
R_{wp}	2.66	2.56	2.63	3.13	3.06
R_{exp}	2.44	1.60	1.59	1.65	1.67
χ^2	1.19	2.56	2.75	3.57	3.38

Table S5. Refined lattice constants, atomic parameters and isotropic thermal parameters of the $Ni_{1-x}Mg_xFe_2O_4$ (x = 0, 0.25, 0.50 0.75 and 1.0).

	$x = 0$	$x = 0.25$	$x = 0.5$	$x = 0.25$	$x = 1.0$
a (Å)	8.32665	8.34682	8.35598	8.36911	8.37994
B_{iso} (A site)	0.761	0.834	1.0	1.0	1.0
B_{iso} (B site)	0.761	1.734	1.0	1.0	1.0
O (x, x, x)	0.25557	0.25694	0.25916	0.25951	0.26169
R_p	2.10	1.69	1.81	1.75	1.72
R_{wp}	2.66	2.46	3.02	2.72	2.75
R_{exp}	2.44	1.57	1.56	1.58	1.58
χ^2	1.19	2.46	3.78	2.95	3.05

Table S6: The positions of the Raman band obtained after deconvolution for the different compositions in $Ni_{1-x}Zn_xFe_2O_4$.

Series		**$Ni_{1-x}Zn_xFe_2O_4$**				
Compositions		***x* = 0.0**	***x* = 0.25**	***x* = 0.50**	***x* = 0.75**	***x* = 1.0**
$A_{1g}(1)$- Fe^{3+}	↑	702.20	704	702.1	698	.....
$A_{1g}(1)$*		660.0	662	661.2	659	.....
$A_{1g}(2)$-Zn^{2+}		.....	636	636.5	638	636
$A_{1g}(2)$*-Zn^{2+}		.....	682	692	684	685
$T_{2g}(3)$-Fe^{3+}		590	580	565	565	545
$T_{2g}(3)$-Ni^{2+}	cm^{-1}	567	560	535	540	.....
$T_{2g}(2)$-Fe^{2+}		493	500	500	505	500
$T_{2g}(2)$-Ni^{2+}		481	486	483	484	.....
$T_{2g}(2)$*-Fe^{2+}		462	477	470	468	
$T_{2g}(2)$*-Ni^{2+}		447	484	450	450	.....
$E_g(1)$-Fe^{3+}/Zn^{2+}		332.2	336	338	340	355
$E_g(2)$*- Zn^{2+}		.....	315	318	315	340
$E_g(1)$*		380	381	377	372	.....
$T_{2g}(1)$	↓	212	200	.....	.....	.....

Table S7: The positions of the Raman band obtained after deconvolution for the different compositions in $Ni_{1-x}Mg_xFe_2O_4$

Series		**$Ni_{1-x}Mg_xFe_2O_4$**				
Compositions		***x* = 0.0**	***x* = 0.25**	***x* = 0.50**	***x* = 0.75**	***x* = 1.0**
$A_{1g}(1)$- Fe^{3+}		702.20	699	705	702	705
$A_{1g}(1)$* - Fe^{3+}		660.0	647	648	643	645
$A_{1g}(2)$-Mg^{2+}		.....	718	720	718	719.20
$A_{1g}(2)$*- Mg^{2+}	cm^{-1}	.....	670	672	673	674
$T_{2g}(3)$-Fe^{3+}		590	563	565	552	545
$T_{2g}(3)$-Ni^{2+}		567	542	548	532	
$T_{2g}(3)$-Mg^{2+}		.....	585	592	570	560
$T_{2g}(2)$-Fe^{2+}		493	482	480	477	475
$T_{2g}(2)$-Ni^{2+}		481	459	460	460	.....
$T_{2g}(2)$- Mg^{2+}		.....	507.6	502	495	500
$T_{2g}(2)$*-Fe^{2+}		462	.....	.....	.....	460
$T_{2g}(2)$*-Ni^{2+}		447	.....	.....	.....	.....
$T_{2g}(2)$*-Mg^{2+}			.....	.....	.....	485
$E_g(1)$- Fe^{3+}/Mg^{2+}		332.2	330	334	330.7	332.74
$E_g(2)$*- Mg^{2+}		.....	303	300	303	300
$E_g(1)$*		380	380	387	375	380.5
$T_{2g}(1)$		212	210	214	214	215
$T_{2g}(1)$*		.....	200	193	203	212

Table S8. The magnetic parameters of the sintered $Ni_{1-x}Mg_xFe_2O_4$ samples.

'x' in $Ni_{1-x}Mg_xFe_2O_4$	M_S (emu/g)	H_C (Oe)	$K_1 \times 10^6$ (erg/cm^3)	T_C (°C)
0	48	55	0.80	592
0.25	40	27	0.19	532
0.5	32	27	0.14	481
0.75	30	25	0.12	415
1	23	25	0.07	368

Table S9. The magnetic parameters of the sintered $Ni_{1-x}Zn_xFe_2O_4$ samples.

'x' in $Ni_{1-x}Zn_xFe_2O_4$	M_S (emu/g)	H_C (Oe)	$K_1 \times 10^6$ (erg/cm^3)	T_C (°C)
0	48	55	0.80	592
0.25	71	16	0.68	431
0.5	74	6	0.58	270
0.75	26 @ 15kOe	-	-	50
1	**Paramagnetic**	-	-	-